Neurobiology of Disease 143 (2020) 104995

Contents lists available at ScienceDirect

Neurobiology of Disease

journal homepage: www.elsevier.com/locate/ynbdi

Delayed administration of the human anti-RGMa monoclonal antibody elezanumab promotes functional recovery including spontaneous voiding after spinal cord injury in rats

Andrea J. Mothe[a,*], Marlon Coelho[a], Lili Huang[b], Philippe P. Monnier[a,e], Yi-Fang Cui[c], Bernhard K. Mueller[c,1], Peer B. Jacobson[d], Charles H. Tator[a,f,*]

[a] Krembil Brain Institute, Toronto Western Hospital, University Health Network, Toronto, ON M5T 0S8, Canada
[b] AbbVie Bioresearch Center, Worcester, MA 01605, USA
[c] Neuroscience Research, AbbVie Deutschland GmbH & Co. KG, Knollstrasse, Ludwigshafen 67061, Germany
[d] Integrated Sciences and Technology, AbbVie, North Chicago, IL 60064-6099, USA
[e] Department of Ophthalmology and Vision Science, University of Toronto, Toronto, ON M5S 3H6, Canada
[f] Department of Surgery, Division of Neurosurgery, University of Toronto, Toronto, ON M5T 2S8, Canada

ARTICLE INFO

Keywords:
Repulsive Guidance Molecule A (RGMa)
Spinal cord injury
Clip impact-compression
Neuronal survival
Axonal plasticity
Bladder function
Elezanumab
ABT-555

ABSTRACT

Spinal cord injury (SCI) often results in permanent functional loss due to a series of degenerative events including cell death, axonal damage, and the upregulation of inhibitory proteins that impede regeneration. Repulsive Guidance Molecule A (RGMa) is a potent inhibitor of axonal growth that is rapidly upregulated following injury in both the rodent and human central nervous system (CNS). Previously, we showed that monoclonal antibodies that specifically block inhibitory RGMa signaling promote neuroprotective and regenerative effects when administered acutely in a clinically relevant rat model of thoracic SCI. However, it is unknown whether systemic administration of RGMa blocking antibodies are effective for SCI after delayed administration. Here, we administered elezanumab, a human monoclonal antibody targeting RGMa, intravenously either acutely or at 3 h or 24 h following thoracic clip impact-compression SCI. Rats treated with elezanumab acutely and at 3 h post-injury showed improvements in overground locomotion and fine motor function and gait. Rats treated 24 h post-SCI trended towards better recovery demonstrating significantly greater stride length and swing speed. Treated rats also showed greater tissue preservation with reduced lesion areas. As seen with acute treatment, delayed administration of elezanumab at 3 h post-SCI also increased perilesional neuronal sparing and serotonergic and corticospinal axonal plasticity. In addition, all elezanumab treated rats showed earlier spontaneous voiding ability and less post-trauma bladder wall hypertrophy. Together, our data demonstrate the therapeutic efficacy of delayed systemic administration of elezanumab in a rat model of SCI, and uncovers a new role for RGMa inhibition in bladder recovery following SCI.

1. Introduction

Traumatic spinal cord injury (SCI) results in a cascade of molecular and degenerative events including apoptosis, axonal damage, and the upregulation of inhibitory molecules which prevent regeneration and limit recovery (Tator and Fehlings, 1991). In the adult CNS, damaged axons fail to regenerate due to several intrinsic and extrinsic factors. Extracellular inhibitory proteins present in myelin such as Nogo-A (Schnell and Schwab, 1990), myelin associated glycoprotein (MAG) (McKerracher et al., 1994), and oligodendrocyte myelin glycoprotein (OMgp) (Wang et al., 2002), together with the accumulation of chondroitin sulfate proteoglycans (Bartus et al., 2012) contribute to the inhibitory environment after SCI, and neutralization of these molecules by various means has improved recovery after SCI (Bregman et al., 1995; Bradbury et al., 2002; Dubreuil et al., 2003; Li et al., 2004).

Repulsive Guidance Molecule A (RGMa) is a potent inhibitor of axonal growth originally identified in the visual system (Monnier et al., 2002), but has also been implicated in neuronal survival, proliferation,

* Corresponding authors at: Krembil Brain Institute, Toronto Western Hospital, University Health Network, Krembil Discovery Tower, 60 Leonard Ave., Toronto, ON M5T 0S8, Canada.
E-mail addresses: andrea.mothe@uhnresearch.ca (A.J. Mothe), charles.tator@uhn.ca (C.H. Tator).
[1] Current address: BMCO, Hannover 30657, Germany.

https://doi.org/10.1016/j.nbd.2020.104995
Received 27 January 2020; Received in revised form 20 May 2020; Accepted 20 June 2020
Available online 23 June 2020

and differentiation (Matsunaga et al., 2004; Niederkofler et al., 2004; Matsunaga et al., 2006; Shifman et al., 2009; Lah and Key, 2012; O'Leary et al., 2013; Chen and Shifman, 2019). RGMa is both membrane bound and secreted (Tassew et al., 2012), and exerts its repulsive activity by binding the Neogenin receptor (Rajagopalan et al., 2004) which requires lipid raft localization for its action to either transmit guidance signals or control cell death (Tassew et al., 2014). RGMa is rapidly upregulated in lesioned areas after traumatic brain injury and SCI in both rodents and humans (Schwab et al., 2005; Hata et al., 2006; Mothe et al., 2017). Moreover, RGMa is also present in multiple sclerosis lesions, ischemic stroke, and amyloid plaques in Alzheimer's disease (Satoh et al., 2013; Demicheva et al., 2015; Shabanzadeh et al., 2015; Zhang et al., 2018). Previous studies have demonstrated the efficacy of inhibiting RGMa with antibodies or other strategies to promote recovery in experimental models of multiple sclerosis (Muramatsu et al., 2011; Demicheva et al., 2015; Tanabe et al., 2018), and an antibody that neutralizes the N-terminal portion of RGMa (ABT-555; elezanumab) is currently being tested in randomized double-blinded phase II trials in patients with relapsing and secondary progressive multiple sclerosis.

Following a bilateral clip impact-compression SCI in rats, we reported a 15-fold upregulation of RGMa primarily expressed in neurons, oligodendrocytes, astrocytes, and activated microglia and macrophages (Mothe et al., 2017). Neutralization of RGMa by acute delivery of C-terminal antibodies via intrathecal catheter and osmotic mini-pumps promoted axonal growth in rats with a thoracic dorsal hemisection of the spinal cord (Hata et al., 2006). Recent studies in monkeys with a unilateral cervical hemisection lesion showed improved manual dexterity and corticospinal tract axonal sprouting with acute intrathecal delivery of C-terminal human RGMa antibodies (Nakagawa et al., 2019). Although these studies demonstrated partial recovery after SCI with RGMa inhibition, the SCI models used have not been clinically relevant; treatment was acute, and the intrathecal route of administration is difficult to translate (Peng and Massicotte, 2004; Hata et al., 2006; Arnold et al., 2011; Nakagawa et al., 2019).

Acute systemic administration of monoclonal antibodies which neutralize RGMa and prevent Neogenin association with lipid rafts thereby inhibiting Neogenin function (Demicheva et al., 2015; Shabanzadeh et al., 2015), promoted neuronal sparing, axonal growth, and functional recovery following a clinically relevant bilateral clip impact-compression thoracic SCI in rats (Mothe et al., 2017). However, it was unknown whether RGMa antibody administration could be delayed to a therapeutically relevant time point after SCI, and therefore, here we used our well-characterized clip impact-compression model with minimally invasive intravenous injections of the antibody to determine the therapeutic time window after SCI for administration of elezanumab.

2. Materials and methods

2.1. RGMa antibodies

The human recombinant RGMa antibody (Ab) used in this study (elezanumab; AbbVie) is a variant of AE12-1Y (Demicheva et al., 2015; Shabanzadeh et al., 2015; Mothe et al., 2017) and an RGMa-selective monoclonal antibody that does not cross-react with the other two RGM family members RGMb and RGMc, as determined by Surface Plasmon Resonance using the BIAcore instrument. Elezanumab exhibits comparable binding affinity to human, cynomolgous macaque, rat and mouse RGMa, and shows a half-life of 7 days as measured using a Mesoscale Discovery (MSD) assay. Various functional assays including chemotaxis, neurite outgrowth, and BMP-responsive reporter gene assays have demonstrated neutralization of RGMa activity with the monoclonal antibodies (Demicheva et al., 2015; Shabanzadeh et al., 2015; Mothe et al., 2017).

2.2. Ethics statement and animals

All animal experiments complied with ARRIVE guidelines. Animal procedures were approved by the Animal Care Committee of the Research Institute of the University Health Network (UHN) in accordance with policies established by the Canadian Council on Animal Care. Efforts were made to minimize the numbers of animals used. All experiments and outcome measures were performed using appropriate blinding. Adult female Wistar rats (Charles River, 280–300 g) were acclimatized and trained for baseline behavioral assessment prior to SCI.

2.3. Spinal cord injury

Amoxicillin (50 mg/kg) was administered in the drinking water 3 days prior to surgery and for 1 week after surgery. Rats were anesthetized by inhalation of 2% isofluorane in oxygen and received subcutaneous injections of buprenorphine (0.05 mg/kg). Rats were positioned in a stereotaxic frame, and aseptic conditions were used for all surgical procedures. With the aid of a surgical microscope, the muscles were retracted to expose the spinous processes and laminae, and a laminectomy was performed at level T8/9. A clip impact-compression injury was made at spinal cord level T8 with a 20 g force by a modified aneurysm clip applied extradurally around the spinal cord to produce a bilateral impact force followed by sustained dorsal-ventral compression for 1 min, a clinically relevant model of SCI reflecting human pathology (Rivlin and Tator, 1978; De Girolami et al., 2002).

2.4. Antibody dosing and animal groups

Rats received an intravenous injection of 25 mg/kg of either elezanumab (AbbVie) antibody (Ab) or human immunoglobulin G (hIgG) control via tail vein at various time intervals after injury. HIgG was recombinantly produced in CHO cells and used as an isotype control (Mothe et al., 2017). SCI rats were randomly allocated to 4 groups: 1) acute elezanumab (acute Ab) (injected < 5 min after injury) ($n = 10$), 2) 3 h elezanumab (3 h Ab) ($n = 9$), 3) 24 h elezanumab (24 h Ab) ($n = 8$), and 4) acute hIgG for control (control) (< 5 min after injury) ($n = 9$). All rats then received weekly tail vein injections for 6 weeks post-SCI at a weekly dose of 25 mg/kg of elezanumab or hIgG control. A summary of the experimental design is shown in Fig. 1A. Age matched normal uninjured rats ($n = 8$) were also used for the bladder analysis and relevant immunostaining data for uninjured spinal cord. For the hIgG tissue staining, 3 rats per group were used.

2.5. Post-operative care

Following SCI, rats received subcutaneous buprenorphine (0.05 mg/kg) for pain control every 12 h for 3 days, and 5 ml subcutaneous saline 2×/day for rehydration for 3 days post-SCI. Amoxicillin (50 mg/kg) was added to the drinking water for 1 week to prevent infection and if required post-SCI due to hematuria or other conditions. Following SCI, all rats experienced weight loss which was gradually regained over the time course. There were no significant differences in weight loss between groups (data not shown). Rats were housed singly in a temperature-controlled room at 26 °C with a 12 h light/dark cycle. Water and food were provided ad libitum.

2.6. Assessment of spontaneous voiding ability

All care and assessments were performed by observers who were blinded as to treatment groups. Bladders were evacuated manually 3 times daily until spontaneous voiding was established. Spontaneous voiding ability was monitored daily in the morning when the bladder is at its fullest. If the bladder was not distended and urine was not expelled during manual bladder expression in the morning, and this

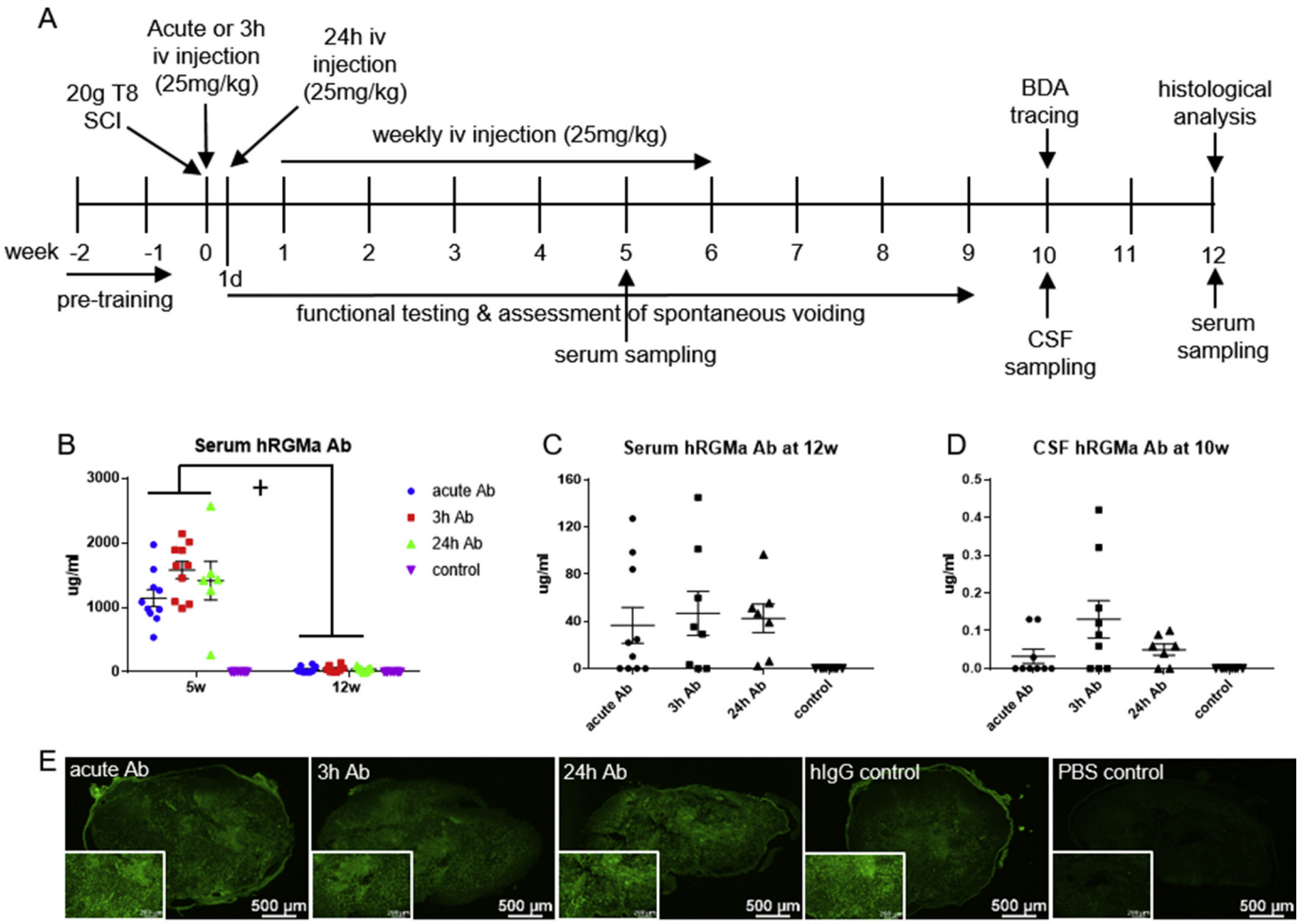

Fig. 1. Summary of experimental design and concentration of elezanumab in serum and CSF and presence in spinal cord tissue. A) Prior to SCI, rats were pre-trained on the locomotor tasks and relevant baseline measurements were obtained. After SCI, rats were injected intravenously (iv) with 25 mg/kg of elezanumab either acutely (< 5 min), or at 3 h or 24 h post-SCI, and then weekly for a total of 6 weeks. Controls were iv injected with hIgG (25 mg/kg) and received the same weekly dosing regimen. Motor and sensory testing and assessment of spontaneous voiding ability was performed over a 9 week period. Serum was collected at 5w and 12w post-SCI and CSF was sampled at 10w post-SCI. BDA was injected into the sensorimotor cortex at 10w for anterograde labeling of the corticospinal tract (CST) and histological analyses were performed at 12w post-SCI. Using an MSD assay, the concentration of elezanumab was measured in B) serum sampled at 5w post-SCI ($n = 10$ for acute Ab, $n = 10$ for 3 h Ab, $n = 6$ for 24 h Ab, $n = 8$ for control) and at 12w post-SCI ($n = 10$ for acute Ab, $n = 8$ for 3 h Ab, $n = 7$ for 24 h Ab, $n = 8$ for control). Serum levels of human RGMa Ab (hRGMa Ab) were significantly elevated at 5w in all Ab treated groups compared to 12w post-SCI ($+p < .0001$). There was no significant differences between groups. However, as shown in the expanded graph (C), RGMa Ab were still detected in serum at 12w post-SCI (6w after the last dose). D) Human RGMa Ab (hRGMa Ab) levels in CSF at 10w post-SCI (4w after the last dose). Data are mean ± SEM ($n = 9$ for acute Ab, $n = 9$ for 3 h Ab, $n = 7$ for 24 h Ab, $n = 8$ for control). E) SCI tissue showed immunostaining for hIgG (green) in all rats injected intravenously with elezanumab and hIgG but not in rats injected with PBS (used as control for staining). (For interpretation of the references to colour in this figure legend, the reader is referred to the web version of this article.)

occurred for 3 consecutive days, the animal was considered to have achieved spontaneous voiding ability. Each rat was scored on a weekly basis as follows: 0, defined as manual voiding of bladder required as rat unable to void on its own; or 1, defined as manual voiding not required as rat able to void on its own.

2.7. Pharmacokinetic analysis with MSD assay

Serum and cerebrospinal fluid (CSF) were collected for determination of the concentration of elezanumab. Serum was collected at 5 weeks post-SCI via saphenous vein sampling and at endpoint at 12 weeks (6 weeks after the last antibody dose) via intracardiac puncture. CSF was sampled at 10 weeks post-SCI (4 weeks after the last antibody dose) via lumbar puncture as we previously described (Mothe et al., 2011; Mothe et al., 2017). The concentration of elezanumab in rat serum and CSF was measured with a MSD assay employing biotinylated elezanumab (1.0 µg/ml) for capture and goat anti-human sulfotag antibody (2.0 µg/ml) for detection. CSF samples were analyzed in 1:100 dilution, and serum samples were analyzed in 1:1000 and 1:5000 dilution at a final matrix concentration of 1%. MSD standard curve fitting and data evaluation was performed using XLfit4 software (Version 4.2.1 Build 16). A calibration curve was plotted from MSD luminescence units versus theoretical standard concentrations. A four-parameter logistic model was used for curve fitting. The regression equation for the calibration curve was then used to back calculate the measured concentrations. The lower limit of quantitation (LLOQ) in the assay was 0.24 ng/ml corresponding to a neat concentration of 1.2 µg/ml (dilution 1:5000) and 0.24 µg/ml (dilution 1:1000) for the serum assay. For the CSF assay (dilution 1:100) the LLOQ in neat matrix was 0.024 µg/ml. The linear range of the standard curve in the serum assay at 1% serum was 0.24–1000 ng/ml. The CSF assay comprised the same standard curve range but was performed in assay buffer and did not contain CSF matrix. Plates were considered valid when at least 2/3 of the quality controls were within 30% of the expected values.

2.8. Functional assessments

Prior to injury rats were trained on the behavioral tests for 2–3 weeks. Functional performance was assessed by several measures: 1) BBB open-field locomotor score for assessment of hind limb function (Basso et al., 1995), 2) motor subscore for additional parameters of overground locomotion (Lankhorst et al., 1999), 3) ladderwalk test for fine motor function and coordination (Metz and Whishaw, 2002), 4) CatWalk system for analysis of gait parameters (Hamers et al., 2001), 5) vonFrey test to assess at-level mechanical allodynia (Bruce et al., 2002), and 6) tail-flick test to evaluate thermal hyperalgesia (Hama and Sagen, 2011). Details of these tests are described below and the experimental design is illustrated in Fig. 1A. All of the outcome measures were performed by two or more blinded testers for 9 weeks after SCI.

2.8.1. BBB locomotor score

Locomotor function was evaluated using the Basso, Beattie and Bresnahan (BBB) open-field locomotor rating scale which ranges from a score of 0 indicating no hind limb movement to 21 indicating normal locomotion as observed in an uninjured rat (Basso et al., 1995). Rats were placed individually in an open field with a non-slippery surface and hind limb motor function including joint movements, stepping ability, coordination, and paw placement were video-recorded for 4 min and scored.

2.8.2. Motor subscore

Additional parameters of overground locomotion were evaluated with the motor subscore scale as previously reported (Lankhorst et al., 1999; Mothe et al., 2017) to assess other measures such as toe clearance, predominant paw position, and trunk stability. A maximal motor subscore of 7 represents normal locomotion.

2.8.3. Ladderwalk test

Fine motor function and coordination were assessed with the horizontal ladderwalk apparatus (Metz and Whishaw, 2002). Rats with a BBB score $>$ 11 were placed on the ladderwalk and at least 3 runs were recorded which were analyzed in slow motion. The total number of footfall errors was scored per hind limb and the total number of hind limb steps was counted. The % hind limb errors was calculated for each run and averaged. Rats unable to perform the test (injured rats with dragging hind limbs) were scored the maximum footfall errors equivalent to 100%. Uninjured rats had 0 or occasionally 1 hind limb footfall per crossing showing an average error of 3%.

2.8.4. CatWalk gait analysis

Gait analysis was assessed using the computerized CatWalk system (Noldus Information Technology, Netherlands) (Hamers et al., 2001). Baseline gait assessments were obtained pre-operatively and compared to assessment at 8 weeks post-SCI. Briefly, the system consists of a horizontal glass plate walkway and video capturing equipment placed underneath the walkway which is connected to a computer. Digital footprints were acquired with the same experimental settings for each rat, and each run was within the required range for crossing time and speed. A minimum of 3 correct crossings (without pausing or interruption) per animal were obtained and digital footprints were labeled and measurements made.

2.8.5. Mechanical allodynia

VonFrey monofilaments (Stoelting) were used to assess cutaneous sensitivity to normally innocuous mechanical stimulation. At-level mechanical allodynia was evaluated by applying 2 g (2 g) and 4 g (4 g) monofilaments to the dermatomes at the level of the SCI as previously described (Bruce et al., 2002; Mothe et al., 2017). Ten mechanical stimuli to the dorsal surface of the trunk around the level of injury at T8 were made in a clock-wise direction starting with the 2 g vonFrey filament. Each stimulus was separated by at least a 5 s interval. Avoidance behavior was defined by one of the following actions: vocalization, flinching, turning away, licking or escaping from the stimulus to another area of the cage. The number of avoidance responses out of 10 was counted to obtain a response percentage.

2.8.6. Thermal hyperalgesia

The tail flick test was used to assess thermal hyperalgesia to evaluate the presence of an exaggerated pain response to noxious stimuli as previously described (Hama and Sagen, 2011; Mothe et al., 2017). An automated analgesia meter (IITC Life Science, Woodland Hills, CA) was used to apply a beam of light to the dorsal surface of the tail at approximately 3 cm from the tip, and the time for the rat to reflexively flick its tail away from the heat stimulus was recorded. Three measurements of tail flick latency were made during a 30 min testing session and averaged.

2.9. Anterograde axonal tracing of the corticospinal tract (CST)

To visualize axons from the CST, anterograde axonal tracing with biotinylated dextran amine (BDA) was performed 10 weeks after SCI following completion of the functional assessments. Animals from each group were randomly selected for BDA injection (n = 4–5). Rats were anesthetized by inhalation of 2% isofluorane in oxygen, and positioned in a stereotaxic frame. As previously described (Tassew et al., 2014; Mothe et al., 2017), the skin was retracted and burr holes were drilled bilaterally at 6 sites overlying each sensorimotor cortex using the following coordinates in reference to bregma: 1) 0.5 mm posterior and 1 mm lateral, 2) 0.5 mm posterior and 2 mm lateral, 3) 1 mm posterior and 1 mm lateral, 4) 1 mm posterior and 2 mm lateral, 5) 1.5 mm posterior and 1 mm lateral, 6) 1.5 mm posterior and 2 mm lateral. BDA (10%, 10,000 MW; #D1956 Invitrogen (Life Technologies)) was dissolved in 0.01 M PBS, and at each site 1 μl of BDA was injected 1.2 mm beneath the surface of the cortex. Injections were made stereotactically with the aid of an operating microscope using a motorized microinjector at a rate of 0.5 μl/min with a 10 μl Hamilton syringe and a 32 gauge needle. The needle was left in place for an additional 2 min after each injection to prevent leakage and the muscle and skin was closed with 3–0 Vicryl. Animals were allowed to survive for 2 more weeks prior to sacrifice.

2.10. Histological assessments

2.10.1. Tissue processing

Rats were sacrificed and transcardially perfused with 4% paraformaldehyde in 0.1 M PBS, pH 7.4 at 12 weeks after SCI after behavioral assessments and anterograde axonal tracing had been performed. Tissue encompassing the lesion site was excised and cryoprotected in 30% sucrose in 0.1 M PBS, embedded in Shandon Cryomatrix (VWR Laboratories) and cryosectioned parasagittally into 20 μm serial sections.

2.10.2. Lesion analysis

For lesion analysis, serial sections were stained with Luxol Fast Blue and hematoxylin and eosin.

(LFB/H&E). the sections were imaged with a Nikon Eclipse Ti microscope (Nikon, Mississauga, ON, Canada) and the lesional area of each section was traced using Nikon NIS Elements BR v.3 software. Any necrotic tissue within the cavities was counted as part the lesion, and the total spinal cord area of the segment was also measured which included 5 mm rostral and caudal to the injury epicenter for a total of 1 cm length of spinal cord. Thus, the lesion area (Area Lesion) and the total spinal cord area (Area Total) were measured. The total lesion volume (Volume Lesion) and total spinal cord volume (Volume Total) were calculated using the Cavalieri method, as previously (Mothe et al., 2017). Briefly, this method is a summation of the measured area of each section multiplied by the inter-section distance. The percentage lesion

area was determined according to the following equation: % Lesion Area = Volume Lesion/Volume Total x 100%.

2.10.3. NeuN Immunostaining and quantification

Serial sections were processed for immunoperoxidase staining for NeuN. Sections were rehydrated in 0.1 M PBS and endogenous peroxidase activity was blocked with 3% H2O2 in methanol for 30 min. Sections were then blocked for 1 h, and incubated overnight at 4 °C with NeuN (1:500, #MAB377 Millipore). Sections were then washed with 0.1 M PBS, incubated with biotinylated anti-mouse secondary antibody (1:500, #BA9200 Vector Laboratories, Burlington, ON, Canada) followed with avidin-biotin-peroxidase complex (Vectastain Elite ABC Kit Standard, #PK6100 Vector Laboratories) for 1 h. Diaminobenzidine (DAB) (Vectastain Elite ABC Kit Standard #PK6100) was applied as the chromogen. To quantify spared host neurons, images were captured with a Nikon Eclipse Ti microscope and cells were manually counted using Nikon NIS Elements BR v.3 software, as previously described (Tassew et al., 2014; Mothe et al., 2017). The sampled region extended from 2.7 mm rostral to 2.7 mm caudal to the lesion epicenter. NeuN+ cells were quantified within the defined region within each consecutive serial section through the volume of the cord. This technique ensured that equivalent gray matter tissue was analyzed in each animal and also avoided double-counting of cells (Mothe et al., 2017). Data are presented as group means of total counts.

2.10.4. 5-HT Immunostaining and quantification

For 5-HT immunohistochemistry, sections were rehydrated in 0.1 M PBS, blocked for 1 h at room temperature in 10% normal goat serum and 0.3% Triton-X, and incubated overnight at 4 °C with anti-5HT antibody (1:3000, #20080 ImmunoStar). Sections were washed with 0.1 M PBS, incubated with goat anti-rabbit A488-conjugated secondary antibody (1:500, #A11034 Invitrogen) for 1 h at room temperature, washed, and then coverslipped with Vectashield mounting medium (#H1200 Vector Laboratories). 5-HT staining was quantified in 3–4 consecutive cross-sections in regions encompassing the ventral horns (2.3×10^4 μm^2 area) in cross-sections 9 mm caudal from the epicenter of the lesion. Immunostained sections were imaged with identical settings and exposure times using a Nikon Eclipse Ti microscope and BR v.3 software and identical threshold settings were applied using ImageJ (NIH) to quantify the % 5-HT+ area of each sampled region and averaged for each cord.

2.10.5. BDA staining and quantification

Following the BDA injections, rats were perfused 2 weeks later as described above and a 1.5 cm segment of tissue encompassing the lesion site was excised and processed as 20 μm serial parasagittal cryosections. In addition, segments of tissue 12 mm and 45 mm rostral to the lesion and a segment of tissue 9 mm caudal to the lesion were cryosectioned transversely. Sections were pre-treated with 1% H2O2 in methanol for 10 min at room temperature, rinsed with PBS (0.1 M, pH 7.4) containing 0.5% Triton-X for 30 min, and incubated in avidin-biotin peroxidase complex (Vectostain Elite ABC Kit Standard, #PK6100 Vector Laboratories), for 1 h at room temperature. Slides were washed with PBS, and then incubated with fluorescent streptavidin Alexa-488 goat anti-mouse secondary antibody (1:500; #S11223 Invitrogen (Life Technologies)) for 1 h at room temperature and coverslipped with Vectashield mounting medium containing DAPI (4′, 6-diamidino-2-phenyl-indole) ((#H1200 Vector Laboratories) nuclear counterstain. Immunofluorescent staining was examined using a Nikon Eclipse Ti microscope. In each cord, cross-sections from the rostral and caudal tissue segments as described above were imaged with identical settings and exposure times. Using ImageJ (NIH), the dorsal corticospinal tract (dCST) was traced and identical threshold settings were applied, and the % BDA+ area was quantified in 4–5 cross-sections for each segment in each cord. The average % BDA+ area of the dCST in the rostral segment (45 mm rostral to the epicenter of the lesion) was used to normalize the values from the other regions of the cord to correct for inter-animal variation in BDA labeling efficiency. The caudal segment was examined for the presence of any BDA labeled fibers. In each cord, 5 consecutive serial sections containing the maximal area of cavitation were used for quantitation. As previously described, the length of BDA fibers was measured from the caudal end of the lesion site and averaged (Mothe et al., 2017). The number of fibers at distances caudal from the lesion site were quantified and binned as follows: < 1000 μm, 1000–2000 μm, > 2000 μm.

2.11. Bladder tissue processing and quantification

Following perfusion, bladders were removed, drained, and weighed to obtain the wet weight. Any bladders that contained stones were not included in the analysis. Bladders were photographed with a ruler and the circumference of each bladder was measured using ImageJ software (NIH) and averaged for each group. The bladders were then fixed in 10% neutral buffered formalin for 2–3 days and a section of the upper portion of the bladder was excised, paraffin processed and embedded. Using a Leica HM 355 S microtome, 5 μm sections were made to visualize the bladder wall. Paraffin sections of the bladders were stained with Verhoeff van Gieson for elastin and collagen. For each bladder, the thickness of the detrusor muscle layer was quantified in 5 sections using Nikon Eclipse Ti microscope and BR v.3 software and averaged for each group.

2.12. Statistical analysis

Quantitative data are presented as the mean ± standard error of the mean (SEM). Data were analyzed with GraphPad Prism (GraphPad Software Inc., La Jolla, CA, USA). Statistical differences between multiple groups were assessed using analysis of variance (ANOVA) and specific post-hoc tests as indicated in the figure legends. Correlation analysis was performed using Pearson product moment correlation. Contingency data was analyzed using chi-square test for trend with post-hoc two-tailed Fisher's exact test. Differences of $p < .05$ were considered to be statistically significant ($*p < .05$, $**p < .01$, $\#p < .001$, $+p < .0001$).

3. Results

3.1. Elezanumab antibodies are detected in rat serum and CSF

Serum was sampled at 5 weeks post-SCI via saphenous vein and at 12 weeks via intracardiac puncture to determine the concentration of elezanumab using a ligand-based assay for human anti-RGMa antibody detection. In addition, CSF samples were obtained at 10 weeks post-SCI via lumbar puncture. As expected, control rats which received hIgG showed no RGMa Ab either in serum or CSF reflecting the specificity of the MSD assay (Fig. 1B–D). Control rats were administered hIgG isotype control recombinantly produced in CHO cells, which differs from high-dose hIgG which is obtained from pooled human sera. Moreover, the dose of hIgG control we used in the present study (25 mg/kg) is only 1.25% the therapeutic dose (2000 mg/kg) of hIgG shown in SCI rats (Chio et al., 2019).

At 5 weeks post-SCI during weekly dosing, very high levels of elezanumab were detected in serum, averaging approximately 1400 μg/ml with no significant difference between groups treated at varying time intervals post-injury (Fig. 1B). By 12 weeks post-SCI or 6 weeks after the last dose, even though serum levels of Ab had significantly declined, elezanumab was detected in 80% of the Ab treated rats (Fig. 1C). Similarly, elezanumab was still detected in the CSF of approximately half the rats at 10 weeks post-SCI even though the CSF was sampled 4 weeks after the last dose was administered, reflecting the stability and longevity of the antibody (Fig. 1D). In addition, we also showed hIgG immunoreactivity at the lesion site following intravenous elezanumab or

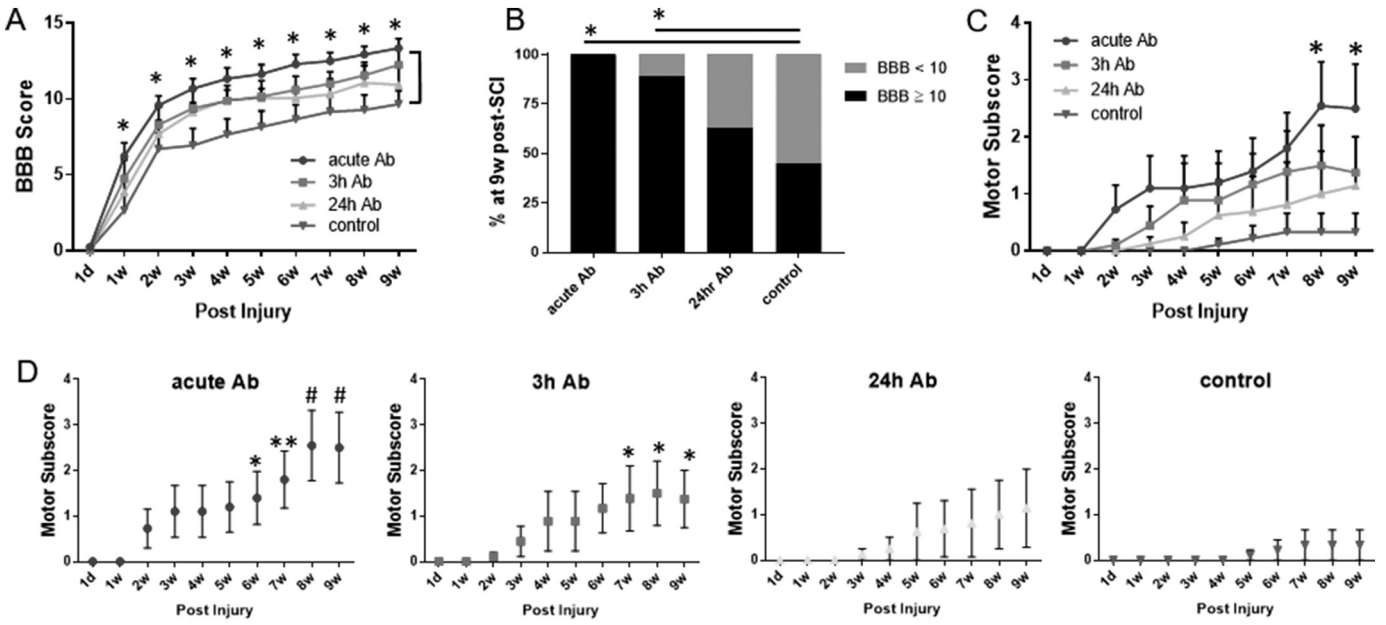

Fig. 2. Delayed treatment with elezanumab promotes recovery in overground locomotion. A) Rats treated with elezanumab showed a higher BBB score after SCI that was statistically significant in the acute group relative to control (acute hIgG) (RM two-way ANOVA, Tukey's multiple comparisons [$F(3,328) = 24.47, p < .05$]). B) The acute and 3 h Ab treated groups showed a significantly higher percentage of animals with BBB scores ≥10 (weight supported stepping) at 9w post-SCI (chi-square test for trend, two-tailed Fisher's exact test, $*p < .05$). C) The Ab treated groups showed a higher motor subscore that was significant in the acute group at 8w and 9w post injury relative to control (RM two-way ANOVA, Tukey's multiple comparisons [$F(3,327) = 11.01, p < .05$]). D) Compared to 1w after injury, only the acute Ab (one-way ANOVA, Dunnett's post-hoc [$F(9,81) = 6.32$], $*p < .05$, $**p < .01$, $\#p < .001$) and 3 h Ab groups (one-way ANOVA, Dunnett's [$F(9,72) = 2.88$], $*p < .05$) showed significant within group recovery. Data are mean ± SEM ($n = 10$ for acute Ab, $n = 9$ for 3 h Ab, $n = 8$ for 24 h Ab, $n = 9$ for control).

hIgG control Ab injection in SCI rats, but not in rats injected with PBS, confirming the presence of antibody penetration into the lesion following systemic administration (Fig. 1E).

3.2. Delayed treatment with RGMa Ab improves fine motor function and gait

Functional recovery was assessed for 9 weeks after SCI using several behavioral tests. On the BBB test, elezanumab (Ab) treated rats showed a trend towards improvement relative to the control group that was statistically significant in the acute group (Fig. 2A). The acute and 3 h elezanumab groups showed a significantly higher percentage of animals with weight supported stepping (BBB scores ≥10) at 9 weeks post-SCI (Fig. 2B). Indeed, 100% of acute Ab and 89% of 3 h Ab rats (Fisher's exact test, $*p < .05$), and 63% of 24 h Ab rats showed weight supported stepping in contrast to only 45% of controls. Similarly, elezanumab treated groups showed a trend towards a higher motor subscore that was significant in the acute group at 8 and 9 weeks post-SCI (Fig. 2C). When compared to 1 week after injury, significant within group recovery was observed only in the acute and 3 h elezanumab treated groups (Fig. 2D). On the ladderwalk test, SCI rats treated with elezanumab showed a lower % of hindlimb footfall errors (acute Ab - 28.6 ± 6.2%; 3 h Ab - 54.3 ± 11.7%; 24 h Ab - 61.9 ± 14.8%) relative to controls (78.4 ± 11.2%) which was significant in the acute Ab group (Fig. 3A). Moreover, when compared to 1 week after injury significant within group recovery was observed only in the acute and 3 h elezanumab treated groups (Fig. 3B). Correlation analysis demonstrated positive correlations between the final BBB scores and serum antibody levels at 5 weeks post-SCI, which was significant in the acute Ab ($r = 0.712, p < .05$) and 3 h Ab ($r = 0.702, p < .05$) groups. There was no correlation with antibody levels and the final motor subscore. However, the % of hindlimb footfall errors negatively correlated with serum antibody levels at 5w post-SCI, although this was not statistically significant (acute Ab, $r = -0.58$; 3 h Ab, $r = -0.65$; 24 h Ab, $r = -0.54$).

Gait parameters were measured pre-SCI and at 8 weeks post-SCI with the CatWalk automated gait assessment system. There were no significant differences between groups in baseline parameters. Normal uninjured rats showed a mean regularity index of 99.1 ± 0.3% reflecting normal coordinated gait which in contrast was impaired after SCI. Rats treated with elezanumab acutely and at 3 h post-SCI showed a significantly higher regularity index (78.0 ± 4.4% and 71.2 ± 3.7%, respectively) relative to controls (50.7 ± 12.8%) reflecting improved inter-paw coordination (Fig. 3C). Stride Length is the distance between successive placements of the same paw which decreases following SCI. Rats treated with elezanumab at all time window intervals showed a greater hindpaw stride length (acute Ab - 12.5 ± 0.51 cm; 3 h Ab - 11.6 ± 1.2 cm; 24 h Ab - 12.8 ± 0.8 cm) relative to controls (9.7 ± 1.8 cm) which was statistically significant in the acute and 24 h groups (Fig. 3D). Swing Speed is the speed of the paw during the swing phase of gait which also decreases after SCI. In contrast, all elezanumab-treated groups showed a significantly higher hindpaw swing speed (Fig. 3E).

We also examined the effect of delayed administration of the RGMa Ab on the development of thermal hyperalgesia and at-level mechanical allodynia after SCI. Thermal hyperalgesia, assessed with the tail-flick test, showed elezanumab-treated rats with increased latency to withdrawal to the heat stimulus, significant in the acute and 24 h Ab groups (Fig. 3F). At-level mechanical allodynia around the lesion site was evaluated with VonFrey filaments which showed fewer adverse responses in the Ab treated groups although there were no significant differences (Fig. 3G,H). Collectively, these results of the functional tests demonstrated improvement with administration of RGMa Ab at 3 h post-injury, whereas the 24 h interval did not show significant functional benefits except in specific gait parameters.

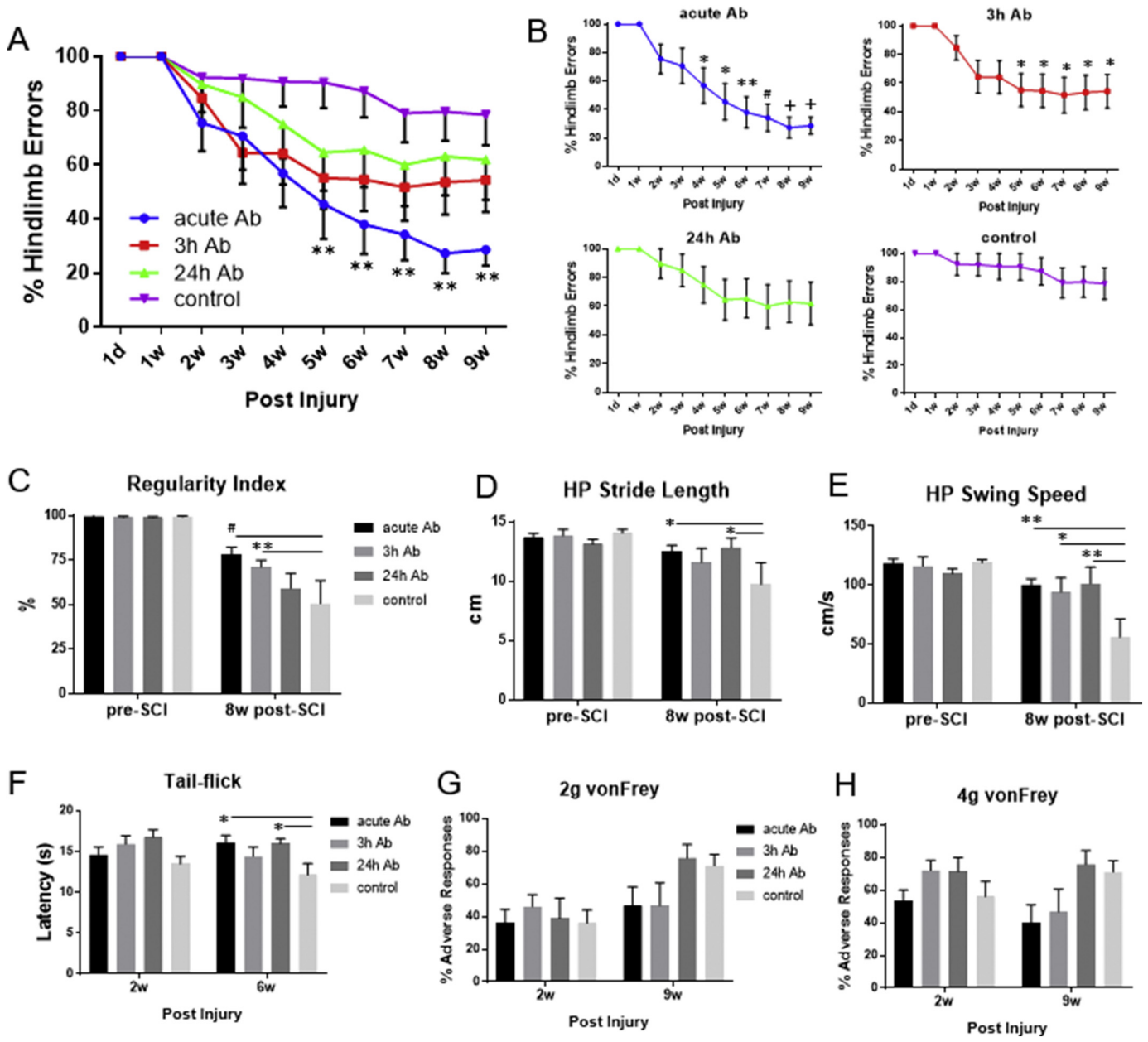

Fig. 3. Delayed treatment with elezanumab improves fine motor function and gait. A) SCI rats treated with elezanumab showed fewer hindlimb footfall errors on the ladderwalk test than the control group and was statistically significant in the acute Ab group (RM two-way ANOVA, Tukey's multiple comparisons [$F(3,320) = 18.21$, $^{**}p < .01$]). B) Compared to 1w after injury, only the acute Ab (one-way ANOVA, Dunnett's post-hoc [$F(9,90) = 8.73$], $^{*}p < .05$, $^{**}p < .01$, $\#p < .001$, $+p < .0001$) and 3 h Ab groups (one-way ANOVA, Dunnett's post-hoc [$F(9,80) = 3.58$], $^{*}p < .05$) showed a significantly lower % of hindlimb footfall errors within each group. Data are mean ± SEM ($n = 10$ for acute Ab, $n = 9$ for 3 h Ab, $n = 8$ for 24 h Ab, $n = 9$ for control). C-E) Gait parameters were obtained by the computerized CatWalk system. C) Rats treated with elezanumab acutely and at 3 h post-SCI showed a significantly higher regularity index relative to controls (two-way ANOVA, Sidak's multiple comparisons [$F(3,59) = 6.11$], $^{**}p < .01$, $\#p < .001$). D) Rats treated at all time window intervals showed a greater hindpaw stride length which was statistically significant in the acute and 24 h groups (two-way ANOVA, Sidak's multiple comparisons [$F(3,59) = 3.01$], $^{*}p < .05$). E) All treated groups showed a significantly higher hindpaw swing speed during the swing phase of gait (two-way ANOVA, Sidak's multiple comparisons [$F(3,59) = 3.14$], $^{*}p < .05$, $^{**}p < .01$). F) Thermal hyperalgesia examined with the tail flick test was reduced in all treated groups, and the acute and 24 h Ab treated rats showed significantly increased latency to withdrawal to the heat stimulus compared to controls (two-way ANOVA, Sidak's multiple comparisons [$F(3,69) = 4.29$], $^{*}p < .05$). G-H) At level mechanical allodynia around the lesion site was evaluated with VonFrey monofilaments. There were no significant differences between groups, although the acute and 3 h Ab groups showed fewer adverse responses compared to controls at 9 weeks with the 2 g (G) and 4 g (H) filament. Data are mean ± SEM ($n = 10$ for acute Ab, $n = 9$ for 3 h Ab, $n = 8$ for 24 h Ab, $n = 9$ for control).

3.3. Neuroprotective effects with delayed administration of elezanumab

The mean percentage lesion area was calculated using LFB/H&E stained sections taking into account the total volume of the spinal cord. Rats treated with elezanumab at all time points showed an approximate 1.5-fold reduction in lesion area compared to controls (Fig. 4). This suggests that inhibition of RGMa after SCI reduces secondary damage and tissue degeneration. The mean lesion area negatively correlated with the final BBB scores although this was not statistically significant.

Acute injection of elezanumab significantly enhanced neuronal survival 9 weeks post-injury with fewer neurons undergoing apoptosis at 7 h post-SCI (Mothe et al., 2017). Rats administered RGMa Ab at 3 h

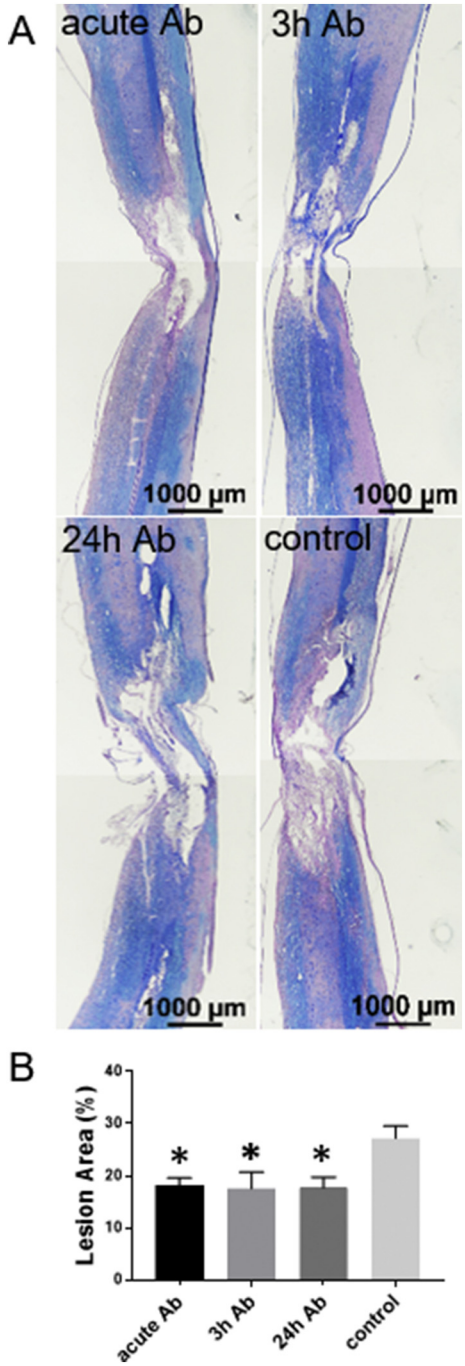

Fig. 4. Reduced lesion area with delayed administration of elezanumab. A) Injured spinal cord stained with LFB/H&E showing the epicenter of the lesion at 12 weeks post-injury. B) The mean % lesion area was quantified taking into account the total volume of the cord. Rats treated with elezanumab showed a significantly reduced lesion area relative to controls (one-way ANOVA, Dunnett's multiple comparisons [$F(3,27) = 4.632$], $^*p < .05$). Data are mean ± SEM ($n = 9$ for acute Ab, $n = 7$ for 3 h Ab, $n = 6$ for 24 h Ab, $n = 9$ for control).

post-SCI also showed a 1.6-fold ($p = .01$) increase in spared perilesional neurons at 12 weeks post-SCI (Fig. 5). When elezanumab administration was delayed to 24 h, there was a 1.5-fold difference in spared neurons relative to controls (approaching significance, $p = .065$), suggesting that the neuroprotective effect of RGMa inhibition is diminished if treatment is delayed to 24 h post-injury. We also found a positive correlation with the number of neurons at 12 weeks post-SCI and serum levels of RGMa antibody at 12 weeks, although this was not statistically significant (acute Ab, $r = 0.81$; 3 h Ab, $r = 0.65$; 24 h Ab, $r = 0.41$).

3.4. Elezanumab enhances axonal plasticity

To visualize axons from the CST, BDA was injected into the sensorimotor cortex and CST tracing analysis was performed at 12 weeks post-SCI. Caudal to the lesion, we found that there were significantly more BDA labeled fibers in Ab treated rats in the acute and 3 h groups and no BDA staining was evident in controls (Fig. 6A,B). We also quantified BDA fibers in the gray matter adjacent to the dorsal corticospinal tract (dCST) in cross-sections 12 mm rostral to the lesion site (Fig. 6C). Interestingly, all RGMa Ab treated rats showed a greater density of BDA+ collaterals in the gray matter compared to untreated controls (Fig. 6D). Moreover, these values were greater than the uninjured value used for normalization, suggesting that there was sprouting of BDA+ CST terminals in the gray matter rostral to the injury following elezanumab administration. We also examined serotonergic innervation of the ventral horn 9 mm caudal to the lesion at 12 weeks post-SCI with 5-HT immunostaining (Fig. 7A). There was significantly greater 5-HT+ staining in the ventral horn in elezanumab-treated rats in the acute and 3 h Ab groups (Fig. 7B).

3.5. RGMa inhibition promotes earlier recovery of spontaneous voiding

Bladder dysfunction following SCI is a common occurrence and is a high priority for SCI patients (Anderson, 2004; Shunmugavel et al., 2015). Similarly, in our clip impact-compression model, rats lose the ability to spontaneously void after SCI and require manual expression of bladders. Hence we examined the time course of spontaneous voiding ability by daily monitoring of each rat and weekly scoring as either requiring or not requiring manual bladder expression depending on whether spontaneous voiding ability had recovered. SCI rats treated with elezanumab showed earlier spontaneous voiding ability compared to the untreated controls (Fig. 8A). At 3 weeks post-SCI, a significantly higher proportion of rats in the acute and 3 h Ab groups showed spontaneous voiding ability relative to controls (Fig. 8B). At 9 weeks post-SCI, 100% of the acute Ab rats, 88.9% of the 3 h Ab rats, and 71.4% of the 24 h Ab rats showed spontaneous voiding ability in comparison to only 22.2% of the controls (Fig. 8C). Examination of the morphological appearance of the bladders at 12 weeks post-SCI showed that the bladder from rats administered elezanumab at all time intervals was smaller than the bladder from untreated controls (Fig. 8D). Quantification of the bladder wet weight showed a trend towards lower bladder weight ($p = .01$ in the 3 h Ab vs. control) approaching the normal small bladder size from uninjured rats (Fig. 8E). In addition, elezanumab-treated rats showed a lower bladder circumference (Fig. 8F). After SCI, the detrusor muscle thickens to compensate for higher bladder pressure resulting from impairment of bladder emptying. We quantified the thickness of the detrusor muscle in the bladder wall in sections stained with Verhoeff van Gieson for elastin and collagen (Fig. 8G) and found that the detrusor muscle was thickest in the bladders from the untreated controls whereas the bladders from elezanumab-treated rats showed a trend towards reduced detrusor muscle thickness (Fig. 8H). Collectively, these data suggest a potential effect of RGMa inhibition on bladder function after SCI.

4. Discussion

This study demonstrates that the time window for elezanumab administration can be extended for at least 3 h after SCI to reduce tissue degeneration, promote neuronal sparing, axonal plasticity, and functional recovery. Improvements in overground locomotion, fine motor function and gait were observed in rats treated acutely and at 3 h post-SCI. However, when administration was delayed to 24 h post-injury, the effects were much smaller except in specific measures of gait,

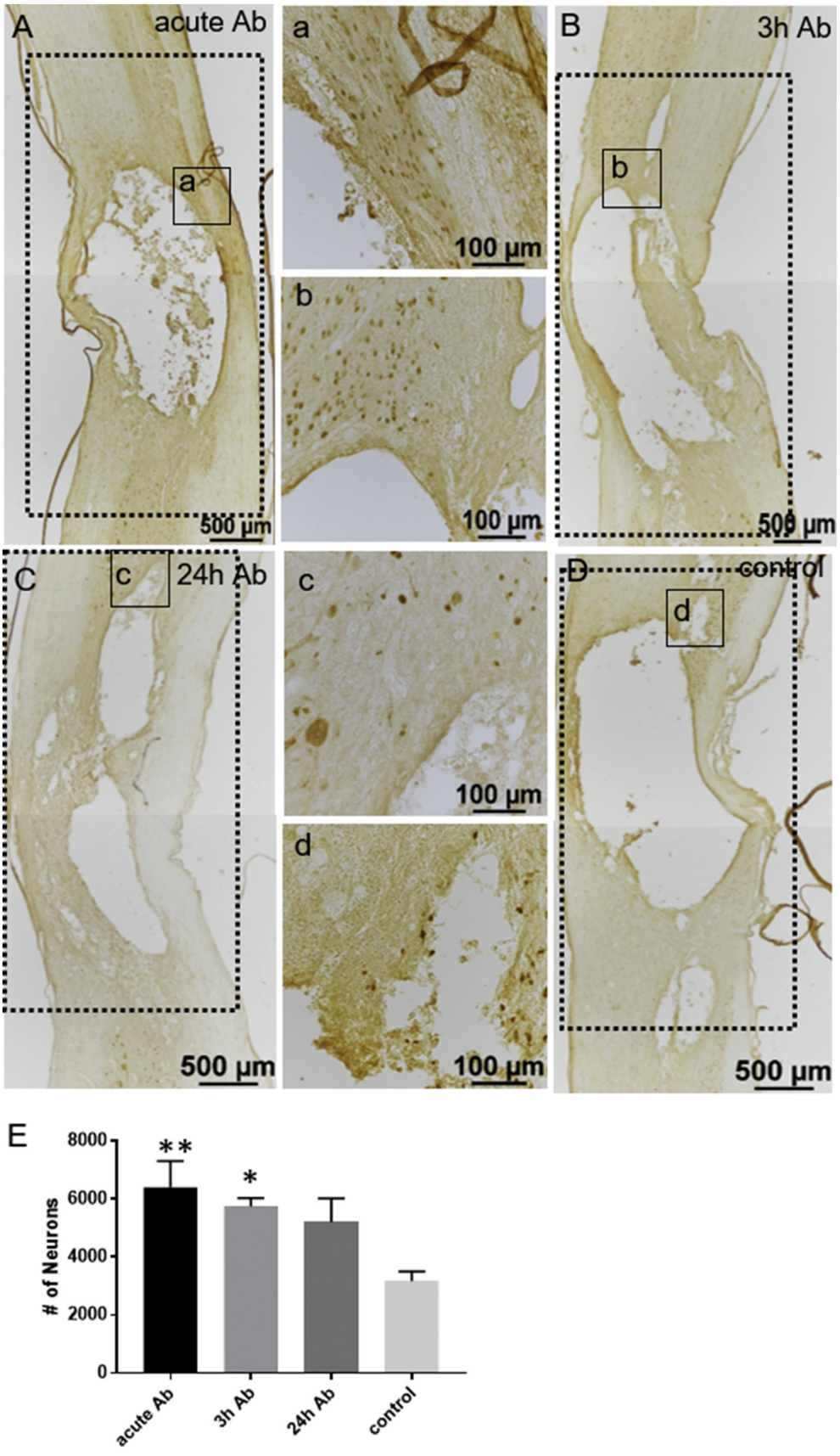

Fig. 5. Delayed administration of elezanumab promotes sparing of perilesional neurons. A-D) Low magnification images of parasagittal sections of injured spinal cord 12 weeks post-SCI immunostained with the neuronal marker NeuN. Solid line boxed regions in each image are magnified in corresponding panels (a-e) showing NeuN + neurons. NeuN + neurons within regions outlined with dotted lines were quantified through the volume of the cord. E) Rats administered elezanumab acutely and at 3 h showed significantly higher perilesional neuronal sparing than controls (one-way ANOVA, Tukey's multiple comparisons [$F(3,22) = 6.75$], $^{*}p < .05$, $^{**}p < .01$). Rats administered Ab 24 h post-SCI showed a trend towards greater neuronal sparing ($p = .065$). Data are mean ± SEM ($n = 6$ per group).

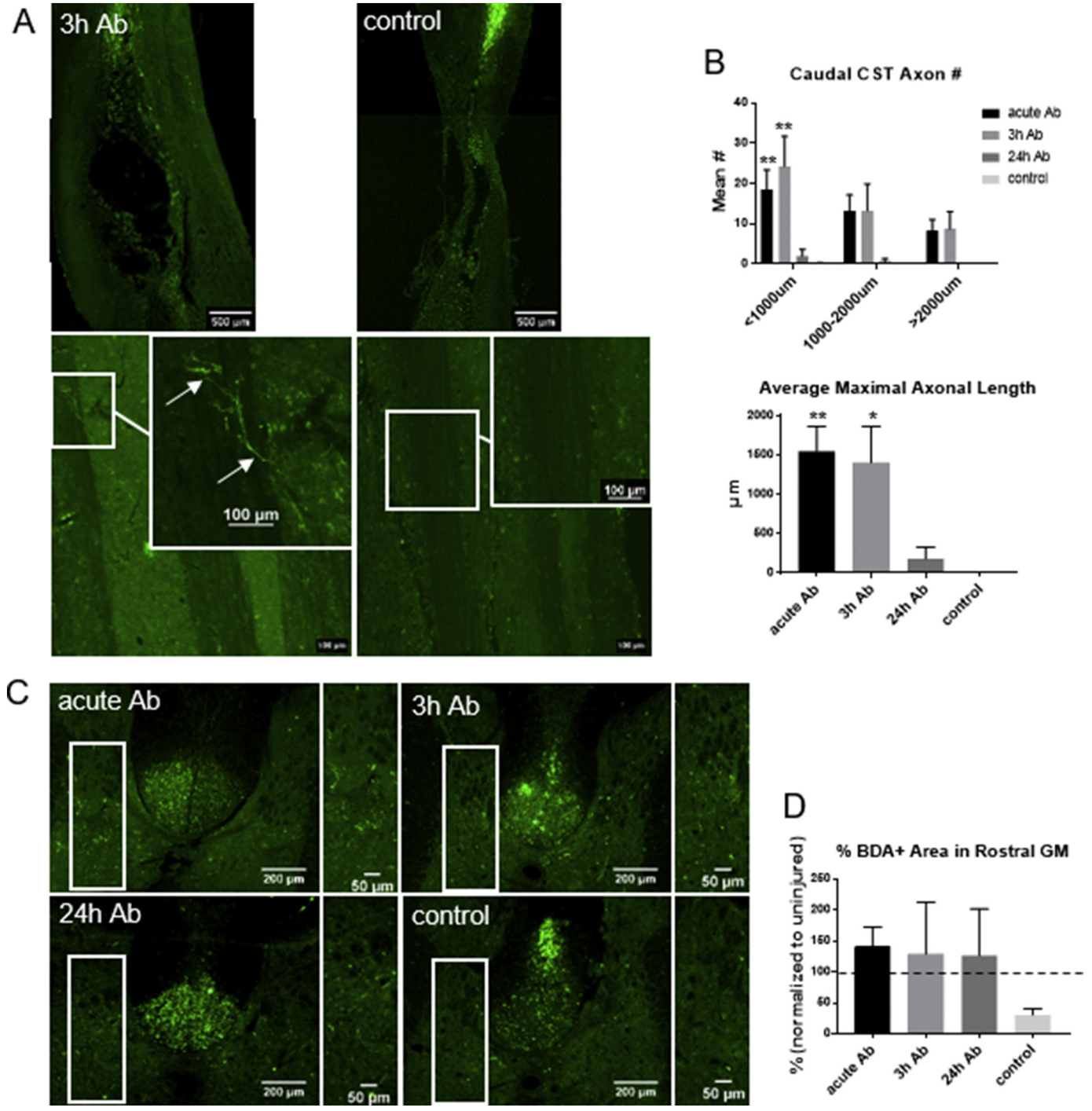

Fig. 6. Elezanumab enhances plasticity of the CST. A) To visualize axons from the CST, BDA was injected at 10 weeks after SCI, and CST tracing analysis was performed at 12 weeks post-SCI. Upper panels show low magnification images of parasagittal sections of spinal cord with rostral orientation at the top showing BDA labeling rostral to the lesion site (shown are 3 h Ab and control). Lower panels show higher magnification images caudal to the lesion site, and boxed regions are shown at higher magnification in the insets. Labeled BDA fibers are seen caudal to the lesion (arrows) in all Ab treated groups but not in control (shown 3 h Ab and control). B) Quantification of the mean CST axon number (two-way ANOVA, Tukey's multiple comparisons [$F(3,37) = 14.76$], $^{**}p < .01$) and average length (one-way ANOVA, Tukey's [$F(3,13) = 9.05$], $^{*}p < .05$, $^{**}p < .01$) of BDA labeled CST fibers showed significantly higher numbers in the acute and 3 h Ab treated groups. Data are mean ± SEM ($n = 4$–5 per group). C) Cross-sections 12 mm rostral to the lesion showing BDA fibers in the gray matter (GM) adjacent to the dorsal corticospinal tract (dCST). The boxed region is shown at higher magnification in the corresponding panels on the right. D) The % area of BDA+ collaterals in the GM adjacent to the dCST within the boxed region shown was quantified. All Ab treated groups showed a trend towards greater % area of BDA+ collaterals in the GM compared to control. % BDA+ area values in all injured groups were normalized to the uninjured value which was considered 100%. Data are mean ± SEM ($n = 4$–5 per group).

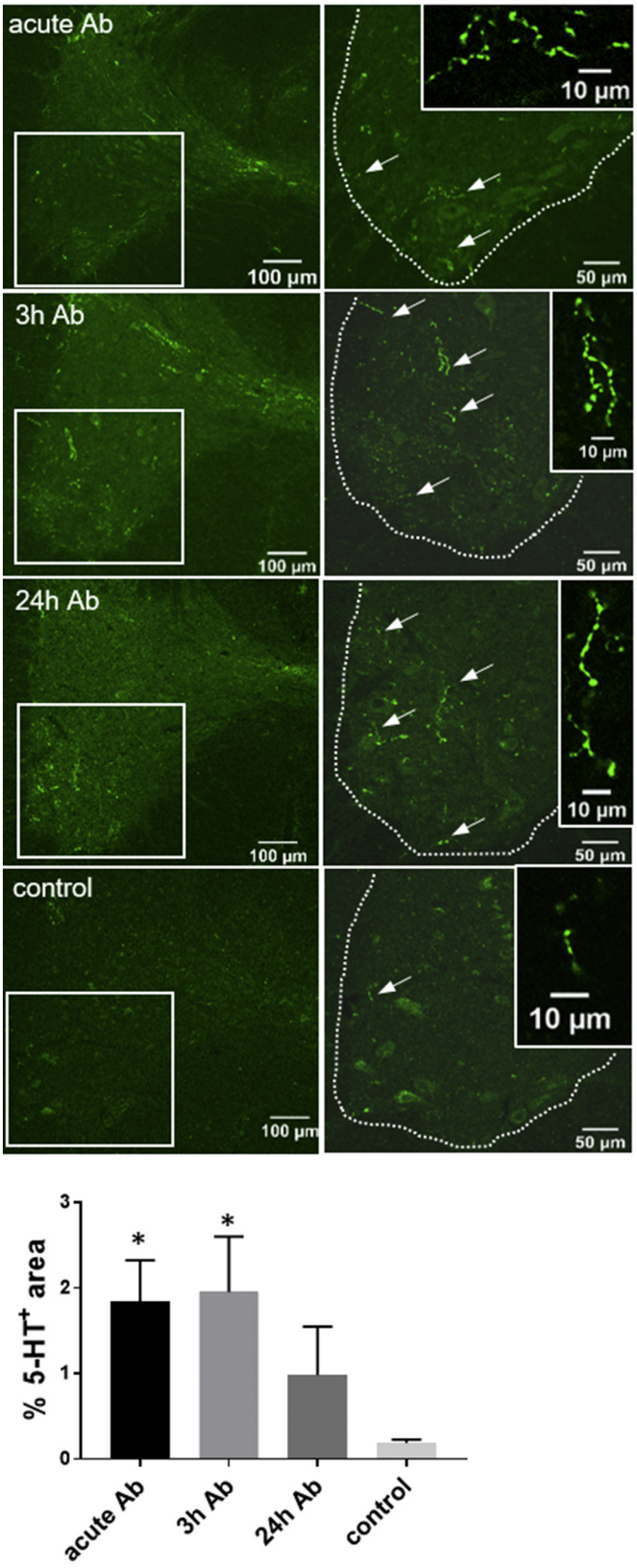

Fig. 7. Elezanumab promotes increased serotonergic innervation of the ventral horn caudal to the lesion. Low magnification images of cross-sections 9 mm caudal from the epicenter of the lesion at 12w post-SCI show 5-HT immunostaining of the gray matter. Boxed regions of the ventral horn are shown at higher magnification in the corresponding panels on the right (dotted outline) showing 5-HT+ fibers (arrows) (control image is overexposed to show staining). Insets show higher magnification of 5-HT+ fibers. 5-HT immunoreactivity was quantified in the ventral horn delineated by the boxed regions. Rats treated with elezanumab showed higher 5-HT immunoreactivity in the ventral horn compared to controls which was statistically significant in the acute and 3 h Ab groups (one-way ANOVA, Dunnett's multiple comparisons [$F(3,14) = 3.49$], $^{*}p < .05$). Data are mean ± SEM ($n = 5$ per group).

suggesting some persisting neuroprotective effects of RGMa inhibition. Indeed, the acute and 3 h treated rats showed significant perilesional neuronal sparing which was also evident at 24 h post-SCI but was not significant. Previously, we showed that N-terminal RGMa antibodies neutralize inhibitory RGMa and block Neogenin function (Demicheva et al., 2015; Shabanzadeh et al., 2015; Mothe et al., 2017). These pleiotropic effects regulated by the N-terminal antibodies reflect the involvement of the Neogenin pathway and the RGMa-BMP pathway (Tian and Liu, 2013; Tassew et al., 2014). For instance, neuroprotective effects with RGMa inhibition have been demonstrated in other experimental paradigms. RGMa antibodies reduced ischemic damage in a stroke model resulting in decreased brain infarct size and improved recovery (Shabanzadeh et al., 2015). Furthermore, we found that elezanumab treatment reduced the lesion area, suggesting neuroprotective effects after thoracic SCI. In the present study, the effect of RGMa inhibition on attenuating secondary damage after injury were significant which may be due to the higher dose of RGMa antibodies used herein.

RGMa is also expressed by other cell types including astrocytes, oligodendrocytes, and microglia and macrophages (Schwab et al., 2005; Hata et al., 2006; Demicheva et al., 2015; Mothe et al., 2017; Tanabe et al., 2018; Zhang et al., 2018). Although the effect of delayed RGMa inhibition on these other cell types was not examined in the present study, this may also contribute to the recovery observed after SCI. Indeed, our previous study showed that SCI rats treated acutely with RGMa antibody showed fewer activated microglia in the dorsal horn caudal to the lesion site (Mothe et al., 2017). In a targeted spinal EAE model of multiple sclerosis, rats treated with RGMa antibody showed decreased CD68+ lesion area, a marker for activated macrophages and microglial cells (Demicheva et al., 2015). RGMa also promotes reactive astrogliosis and glial scar formation via TGFβ1/Smad2/3 signaling which was attenuated with RGMa knockdown or pharmacological inhibition of RGMa in a rat model of stroke (Zhang et al., 2018).

The present study shows that elezanumab administered at 3 h post-injury enhanced sprouting of serotonergic and CST axons. However, despite weekly dosing, when the administration was delayed to 24 h there was only a small number of BDA labeled CST fibers caudal to the lesion site. This may be because the CST is known to be highly refractory to regeneration and may be more susceptible to retrograde degeneration. Additionally, the severity of the clip impact-compression injury used in the present study results in extensive cystic cavitation (Rivlin and Tator, 1978), and without additional strategies to induce axonal regeneration, the potential for regeneration beyond the lesion site is less compared to partial lesion models (Fry et al., 2010). In contrast, rostral to the thoracic lesion site, we found equivalent levels of CST sprouting in the cervical gray matter of elezanumab-treated rats at all time window intervals. Following thoracic hemisection in SCI rats, RGMa inhibition promoted synapse formation of spared CST axonal projections in the cervical region (Kyoto et al., 2007). We also found greater serotonergic innervation of the ventral horn caudal to the lesion site following delayed antibody treatment, suggesting enhanced serotonergic axonal plasticity with RGMa inhibition.

In terms of extrapolation of post-injury time windows from rodent to human there is no accepted direct equation one can apply, however indirect information based on metabolic rate differences suggest that the pathological changes occurring at 1 h after SCI in rats are approximately equivalent to 4 h post-injury in humans (Wu et al., 2013). Moreover, studies examining inflammatory biomarkers after SCI in

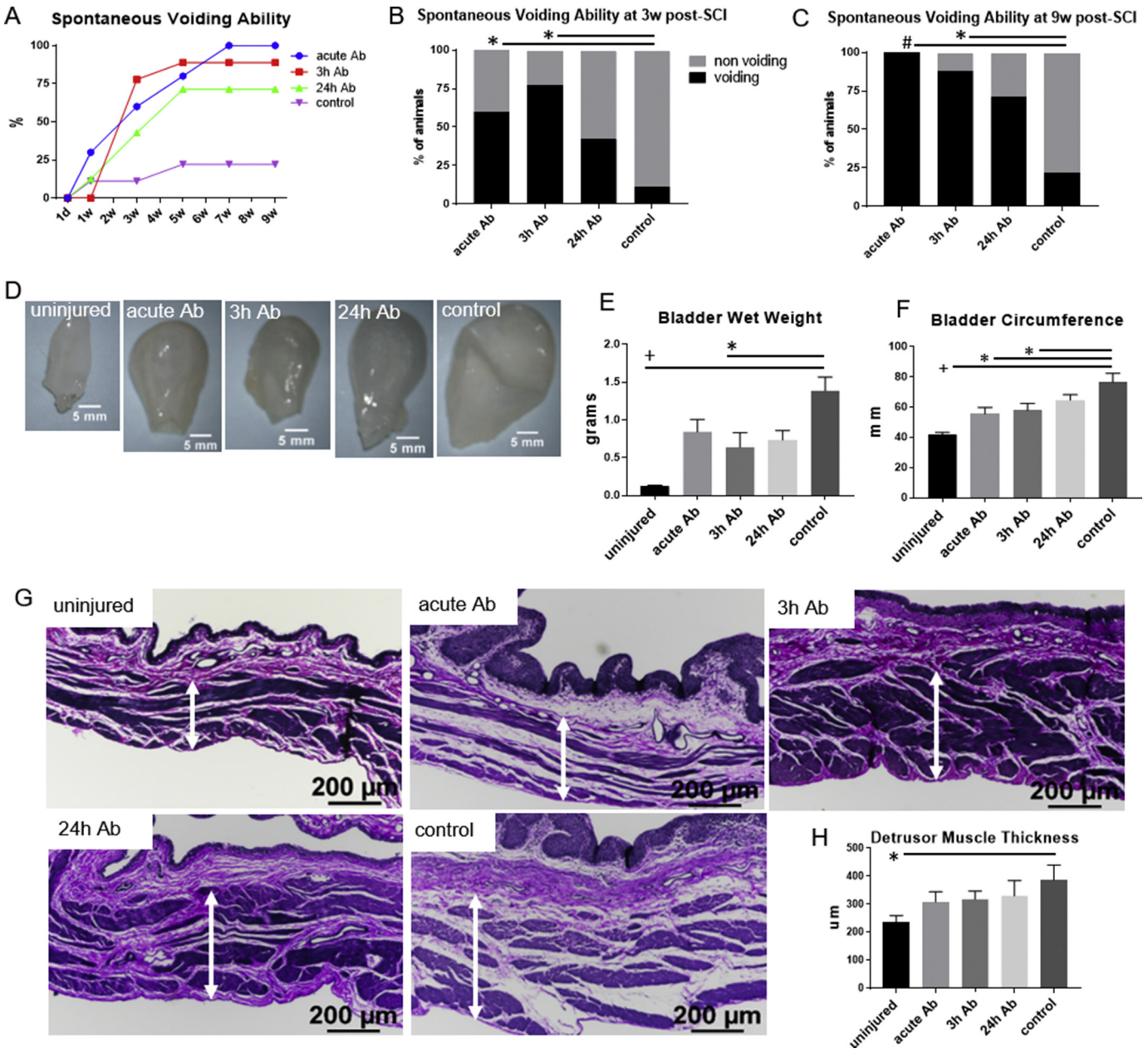

Fig. 8. RGMa inhibition promotes earlier recovery of spontaneous voiding. A) SCI rats treated with elezanumab showed earlier spontaneous voiding ability from 2w onwards after injury, as shown in the time course graph. B) At 3w post-SCI, a significantly higher proportion of rats in the acute and 3 h Ab groups showed spontaneous voiding ability compared to the control group (chi-square test for trend, two-tailed Fisher's exact test, $*p < .05$). C) At 9w post-SCI, 100% of the acute Ab rats, 88.9% of the 3 h Ab rats, and 71.4% of the 24 h Ab rats showed spontaneous voiding ability which was significantly greater in the acute and 3 h Ab groups relative to controls (22.2%) (two-tailed Fisher's exact test, $*p < .05$, $\#p < .001$). D) The morphological appearance of the bladders from 12w post-SCI rats were larger than from uninjured normal rats. E) The bladders from all elezanumab-treated rats showed a lower bladder weight relative to controls (SCI rats treated with hIgG), which was statistically significant in the 3 h Ab and uninjured groups compared to controls (one-way ANOVA, Tukey's [$F(4,34) = 8.67$], $*p < .05$, $+p < .0001$). F) The bladders from the uninjured rats and the acute and 3 h Ab treated rats showed a significantly lower bladder circumference relative to control rats (one-way ANOVA, Tukey's [$F(4,33) = 9.14$], $*p < .05$, $+p < .0001$). G) Bladder tissue from 12w post-SCI rats was stained with Verhoeff van Gieson for elastin and collagen, and the thickness of the detrusor muscle (white arrows) was measured. H) Ab treated rats showed a trend towards lower detrusor muscle thickness of the bladder closer to the bladders of uninjured rats. The detrusor muscle thickness of the bladder was significantly less in the uninjured rats relative to SCI controls (one-way ANOVA, Tukey's [$F(4,33) = 2.75$], $*p < .05$). Rats with bladder stones were excluded from all analyses ($n = 10$ for acute Ab, $n = 7$ for 3 h Ab, $n = 6$ for 24 h Ab, $n = 8$ for control).

rodents and human patients suggest many biomarkers peak earlier at approximately 4 h post-SCI in rodents compared to 24 h–32 h after SCI in humans (Kwon et al., 2010; Stammers et al., 2012). These comparisons suggest an approximate difference of 4–8 h between rodent and human SCI pathology. Accordingly, a 3 h post-injury time window in rat would be roughly equivalent to 12-24 h in human which is clinically important because it provides enough time for most SCI patients to reach treatment centres, and to begin treatment. Furthermore, it is conceivable that an intermediate time window of antibody administration between 3 h and 24 h post-SCI would be equally effective. For instance, RGMa antibodies administrated 6 h after middle cerebral artery occlusion in an animal model of stroke produced functional improvements (Shabanzadeh et al., 2015). Thus, administration of RGMa antibodies following thoracic SCI can potentially be extended for at

least 3 h after injury in the rat which is a more clinically relevant administration timepoint and an important extension of what was previously known.

The other important finding from the present study relates to post injury recovery of bladder function. Micturition is regulated by several pathways in the brain, spinal cord, and peripheral ganglia. Diseases or injuries to the CNS often cause loss of voluntary bladder and bowel emptying leading to a large range of complications including bladder and bowel incontinence. Indeed, more than 80% of SCI patients show micturition/voiding dysfunction (Shunmugavel et al., 2015), as supraspinal pathways modulating bladder function are often interrupted. These deficits are of immense importance to patients with SCI and can lead to major urinary tract infection, with severe morbidity and even mortality. Interestingly, we found that elezanumab treatment at all time intervals induced much earlier onset of spontaneous voiding ability. In particular, a significantly higher proportion of rats treated acutely and at 3 h post-injury were able to spontaneously void compared to untreated SCI rats. Furthermore, we found that bladders from treated rats at 12w post-SCI were smaller with a lower weight and circumference than untreated SCI controls, more closely resembling bladders from uninjured rats. Thus, the effect of RGMa inhibition on bladder recovery after SCI should be investigated further. Indeed, a recent study showed that 2 weeks of acute intrathecal anti-Nogo-A antibody treatment to SCI rats significantly improved bladder function (Schneider et al., 2019).

5. Conclusions

These preclinical data suggest that the window of administration for a systemic RGMa antibody can be extended to the subacute stage of thoracic SCI. The effects of systemic RGMa inhibition are still evident for at least 3 h after injury in terms of functional improvements, reduced lesion area, neuronal protection, and increased axonal plasticity of CST and serotonergic fibers. Extending the time of administration to 24 h post-SCI did not show significant tissue and functional benefits except in specific gait parameters. Furthermore, we showed for the first time beneficial effects of elezanumab after SCI on restoration of spontaneous voiding function and improved bladder morphology which warrants further investigation.

Acknowledgments

We are grateful for funding support from the Wings for Life Spinal Cord Research Foundation, Canadian Institutes of Health Research, AbbVie, Toronto General and Western Hospital Foundation, Jericho Foundation, and Spinal Cord Injury Ontario. We thank Carmin Szynal and Christine Grinnell from Abbvie Bioresearch Center for their technical assistance. We thank Rita van Bendegem and Linda Lee for their technical expertise in animal care, functional testing, and tissue processing. We thank Shalom Halbert for help with tissue analysis, and the veterinarians and staff at the Animal Resource Centre at UHN.

Author disclosure statement

The RGMa antibody was developed by AbbVie and is the property of this company which owns all the rights and commercial interests on the use of this antibody. L.H, Y·C, and P.J are employees of AbbVie and may hold stock/stock options. B.K.M is a previous AbbVie employee. Financial support for this research was provided in part by AbbVie. AbbVie participated in the analyses of the MSD data and in the review and approval of the manuscript. No other competing financial interests exist.

References

Anderson, K.D., 2004. Targeting recovery: priorities of the spinal cord-injured population. J. Neurotrauma 21, 1371–1383.

Arnold, P.M., Harsh, V., Oliphant, S.M., 2011. Spinal cord compression secondary to intrathecal catheter-induced granuloma: a report of four cases. Evid. Based Spine Care J. 2, 57–62.

Bartus, K., James, N.D., Bosch, K.D., Bradbury, E.J., 2012. Chondroitin sulphate proteoglycans: key modulators of spinal cord and brain plasticity. Exp. Neurol. 235, 5–17.

Basso, D.M., Beattie, M.S., Bresnahan, J.C., 1995. A sensitive and reliable locomotor rating scale for open field testing in rats. J. Neurotrauma 12, 1–21.

Bradbury, E.J., Moon, L.D., Popat, R.J., King, V.R., Bennett, G.S., Patel, P.N., Fawcett, J.W., McMahon, S.B., 2002. Chondroitinase ABC promotes functional recovery after spinal cord injury. Nature 416, 636–640.

Bregman, B.S., Kunkel-Bagden, E., Schnell, L., Dai, H.N., Gao, D., Schwab, M.E., 1995. Recovery from spinal cord injury mediated by antibodies to neurite growth inhibitors. Nature 378, 498–501.

Bruce, J.C., Oatway, M.A., Weaver, L.C., 2002. Chronic pain after clip-compression injury of the rat spinal cord. Exp. Neurol. 178, 33–48.

Chen, J., Shifman, M.I., 2019. Inhibition of neogenin promotes neuronal survival and improved behavior recovery after spinal cord injury. Neuroscience 408, 430–447.

Chio, J.C.T., Wang, J., Badner, A., Hong, J., Surendran, V., Fehlings, M.G., 2019. The effects of human immunoglobulin G on enhancing tissue protection and neurobehavioral recovery after traumatic cervical spinal cord injury are mediated through the neurovascular unit. J. Neuroinflammation 16, 141.

De Girolami, U., Frosch, M.P., Tator, C.H., 2002. Diseases of the spinal cord and vertebral column. In: Graham, D.I., Lantos, P. (Eds.), Greenfield's Neuropathology 7th Edition, Regional Neuropathology. Arnold Publishers, London, England, pp. 1063–1101.

Demicheva, E., et al., 2015. Targeting repulsive guidance molecule A to promote regeneration and neuroprotection in multiple sclerosis. Cell Rep. 10, 1887–1898.

Dubreuil, C.I., Winton, M.J., McKerracher, L., 2003. Rho activation patterns after spinal cord injury and the role of activated Rho in apoptosis in the central nervous system. J. Cell Biol. 162, 233–243.

Fry, E.J., Chagnon, M.J., Lopez-Vales, R., Tremblay, M.L., David, S., 2010. Corticospinal tract regeneration after spinal cord injury in receptor protein tyrosine phosphatase sigma deficient mice. Glia 58, 423–433.

Hama, A., Sagen, J., 2011. Antinociceptive effect of riluzole in rats with neuropathic spinal cord injury pain. J. Neurotrauma 28, 127–134.

Hamers, F.P., Lankhorst, A.J., van Laar, T.J., Veldhuis, W.B., Gispen, W.H., 2001. Automated quantitative gait analysis during overground locomotion in the rat: its application to spinal cord contusion and transection injuries. J. Neurotrauma 18, 187–201.

Hata, K., Fujitani, M., Yasuda, Y., Doya, H., Saito, T., Yamagishi, S., Mueller, B.K., Yamashita, T., 2006. RGMa inhibition promotes axonal growth and recovery after spinal cord injury. J. Cell Biol. 173, 47–58.

Kwon, B.K., Stammers, A.M., Belanger, L.M., Bernardo, A., Chan, D., Bishop, C.M., Slobogean, G.P., Zhang, H., Umedaly, H., Giffin, M., Street, J., Boyd, M.C., Paquette, S.J., Fisher, C.G., Dvorak, M.F., 2010. Cerebrospinal fluid inflammatory cytokines and biomarkers of injury severity in acute human spinal cord injury. J. Neurotrauma 27, 669–682.

Kyoto, A., Hata, K., Yamashita, T., 2007. Synapse formation of the cortico-spinal axons is enhanced by RGMa inhibition after spinal cord injury. Brain Res. 1186, 74–86.

Lah, G.J., Key, B., 2012. Dual roles of the chemorepellent axon guidance molecule RGMa in establishing pioneering axon tracts and neural fate decisions in embryonic vertebrate forebrain. Dev. Neurobiol. 72, 1458–1470.

Lankhorst, A.J., Duis, S.E., ter Laak, M.P., Joosten, E.A., Hamers, F.P., Gispen, W.H., 1999. Functional recovery after central infusion of alpha-melanocyte-stimulating hormone in rats with spinal cord contusion injury. J. Neurotrauma 16, 323–331.

Li, S., Liu, B.P., Budel, S., Li, M., Ji, B., Walus, L., Li, W., Jirik, A., Rabacchi, S., Choi, E., Worley, D., Sah, D.W., Pepinsky, B., Lee, D., Relton, J., Strittmatter, S.M., 2004. Blockade of Nogo-66, myelin-associated glycoprotein, and oligodendrocyte myelin glycoprotein by soluble Nogo-66 receptor promotes axonal sprouting and recovery after spinal injury. J. Neurosci. 24, 10511–10520.

Matsunaga, E., Tauszig-Delamasure, S., Monnier, P.P., Mueller, B.K., Strittmatter, S.M., Mehlen, P., Chedotal, A., 2004. RGM and its receptor neogenin regulate neuronal survival. Nat. Cell Biol. 6, 749–755.

Matsunaga, E., Nakamura, H., Chedotal, A., 2006. Repulsive guidance molecule plays multiple roles in neuronal differentiation and axon guidance. J. Neurosci. 26, 6082–6088.

McKerracher, L., David, S., Jackson, D.L., Kottis, V., Dunn, R.J., Braun, P.E., 1994. Identification of myelin-associated glycoprotein as a major myelin-derived inhibitor of neurite growth. Neuron 13, 805–811.

Metz, G.A., Whishaw, I.Q., 2002. Cortical and subcortical lesions impair skilled walking in the ladder rung walking test: a new task to evaluate fore- and hindlimb stepping, placing, and co-ordination. J. Neurosci. Methods 115, 169–179.

Monnier, P.P., Sierra, A., Macchi, P., Deitinghoff, L., Andersen, J.S., Mann, M., Flad, M., Hornberger, M.R., Stahl, B., Bonhoeffer, F., Mueller, B.K., 2002. RGM is a repulsive guidance molecule for retinal axons. Nature 419, 392–395.

Mothe, A.J., Bozkurt, G., Catapano, J., Zabojova, J., Wang, X., Keating, A., Tator, C.H., 2011. Intrathecal transplantation of stem cells by lumbar puncture for thoracic spinal cord injury in the rat. Spinal Cord 49, 967–973.

Mothe, A.J., Tassew, N.G., Shabanzadeh, A.P., Penheiro, R., Vigouroux, R.J., Huang, L., Grinnell, C., Cui, Y.F., Fung, E., Monnier, P.P., Mueller, B.K., Tator, C.H., 2017. RGMa inhibition with human monoclonal antibodies promotes regeneration, plasticity and repair, and attenuates neuropathic pain after spinal cord injury. Sci. Rep. 7, 10529.

Muramatsu, R., Kubo, T., Mori, M., Nakamura, Y., Fujita, Y., Akutsu, T., Okuno, T., Taniguchi, J., Kumanogoh, A., Yoshida, M., Mochizuki, H., Kuwabara, S., Yamashita, T., 2011. RGMa modulates T cell responses and is involved in autoimmune encephalomyelitis. Nat. Med. 17, 488–494.

Nakagawa, H., Ninomiya, T., Yamashita, T., Takada, M., 2019 Feb 1. Treatment with the neutralizing antibody against repulsive guidance molecule-a promotes recovery from impaired manual dexterity in a primate model of spinal cord injury. Cereb. Cortex 29 (2), 561–572. https://doi.org/10.1093/cercor/bhx338.

Niederkofler, V., Salie, R., Sigrist, M., Arber, S., 2004. Repulsive guidance molecule (RGM) gene function is required for neural tube closure but not retinal topography in the mouse visual system. J. Neurosci. 24, 808–818.

O'Leary, C., Cole, S.J., Langford, M., Hewage, J., White, A., Cooper, H.M., 2013. RGMa regulates cortical interneuron migration and differentiation. PLoS One 8, e81711.

Peng, P., Massicotte, E.M., 2004. Spinal cord compression from intrathecal catheter-tip inflammatory mass: case report and a review of etiology. Reg. Anesth. Pain Med. 29, 237–242.

Rajagopalan, S., Deitinghoff, L., Davis, D., Conrad, S., Skutella, T., Chedotal, A., Mueller, B.K., Strittmatter, S.M., 2004. Neogenin mediates the action of repulsive guidance molecule. Nat. Cell Biol. 6, 756–762.

Rivlin, A.S., Tator, C.H., 1978. Effect of duration of acute spinal cord compression in a new acute cord injury model in the rat. Surg. Neurol. 10, 38–43.

Satoh, J., Tabunoki, H., Ishida, T., Saito, Y., Arima, K., 2013. Accumulation of a repulsive axonal guidance molecule RGMa in amyloid plaques: a possible hallmark of regenerative failure in Alzheimer's disease brains. Neuropathol. Appl. Neurobiol. 39, 109–120.

Schneider, M.P., Sartori, A.M., Ineichen, B.V., Moors, S., Engmann, A.K., Hofer, A.S., Weinmann, O., Kessler, T.M., Schwab, M.E., 2019. Anti-Nogo-A antibodies as a potential causal therapy for lower urinary tract dysfunction after spinal cord injury. J. Neurosci. 39, 4066–4076.

Schnell, L., Schwab, M.E., 1990. Axonal regeneration in the rat spinal cord produced by an antibody against myelin-associated neurite growth inhibitors. Nature 343, 269–272.

Schwab, J.M., Conrad, S., Monnier, P.P., Julien, S., Mueller, B.K., Schluesener, H.J., 2005. Spinal cord injury-induced lesional expression of the repulsive guidance molecule (RGM). Eur. J. Neurosci. 21, 1569–1576.

Shabanzadeh, A.P., Tassew, N.G., Szydlowska, K., Tymianski, M., Banerjee, P., Vigouroux, R.J., Eubanks, J.H., Huang, L., Geraerts, M., Koeberle, P.D., Mueller, B.K., Monnier, P.P., 2015. Uncoupling Neogenin association with lipid rafts promotes neuronal survival and functional recovery after stroke. Cell Death Dis. 6, e1744.

Shifman, M.I., Yumul, R.E., Laramore, C., Selzer, M.E., 2009. Expression of the repulsive guidance molecule RGM and its receptor neogenin after spinal cord injury in sea lamprey. Exp. Neurol. 217, 242–251.

Shunmugavel, A., Khan, M., Hughes Jr., F.M., Purves, J.T., Singh, A., Singh, I., 2015. S-Nitrosoglutathione protects the spinal bladder: novel therapeutic approach to post-spinal cord injury bladder remodeling. Neurourol. Urodyn. 34, 519–526.

Stammers, A.T., Liu, J., Kwon, B.K., 2012. Expression of inflammatory cytokines following acute spinal cord injury in a rodent model. J. Neurosci. Res. 90, 782–790.

Tanabe, S., Fujita, Y., Ikuma, K., Yamashita, T., 2018. Inhibiting repulsive guidance molecule-a suppresses secondary progression in mouse models of multiple sclerosis. Cell Death Dis. 9, 1061.

Tassew, N.G., Charish, J., Seidah, N.G., Monnier, P.P., 2012. SKI-1 and Furin generate multiple RGMa fragments that regulate axonal growth. Dev. Cell 22, 391–402.

Tassew, N.G., Mothe, A.J., Shabanzadeh, A.P., Banerjee, P., Koeberle, P.D., Bremner, R., Tator, C.H., Monnier, P.P., 2014. Modifying lipid rafts promotes regeneration and functional recovery. Cell Rep. 8, 1146–1159.

Tator, C.H., Fehlings, M.G., 1991. Review of the secondary injury theory of acute spinal cord trauma with emphasis on vascular mechanisms. J. Neurosurg. 75, 15–26.

Tian, C., Liu, J., 2013. Repulsive guidance molecules (RGMs) and neogenin in bone morphogenetic protein (BMP) signaling. Mol. Reprod. Dev. 80, 700–717.

Wang, K.C., Kim, J.A., Sivasankaran, R., Segal, R., He, Z., 2002. P75 interacts with the Nogo receptor as a co-receptor for Nogo, MAG and OMgp. Nature 420, 74–78.

Wu, Y., Satkunendrarajah, K., Teng, Y., Chow, D.S., Buttigieg, J., Fehlings, M.G., 2013. Delayed post-injury administration of riluzole is neuroprotective in a preclinical rodent model of cervical spinal cord injury. J. Neurotrauma 30, 441–452.

Zhang, R., Wu, Y., Xie, F., Zhong, Y., Wang, Y., Xu, M., Feng, J., Charish, J., Monnier, P.P., Qin, X., 2018. RGMa mediates reactive astrogliosis and glial scar formation through TGFbeta1/Smad2/3 signaling after stroke. Cell Death Differ. 25, 1503–1516.